ChemPubSoc Europe

DOI: 10.1002/cmdc.201400056

VIP

Cytotoxic Gold(I) N-heterocyclic Carbene Complexes with Phosphane Ligands as Potent Enzyme Inhibitors

Riccardo Rubbiani,[a] Luca Salassa,[b, c] Andreia de Almeida,[d] Angela Casini,[d] and Ingo Ott*[a]

Organometallic gold complexes with N-heterocyclic carbene (NHC) ligands have been demonstrating promising properties as novel anticancer agents. Gold(I) NHC complexes containing different phosphanes as secondary ligands were shown to trigger strong cytotoxic effects in cancer cells, and their effective uptake into the cells was quantified by atomic absorption spectroscopy. Moreover, the new compounds strongly inhibited the activity of the seleno-enzyme thioredoxin reductase (TrxR) and of the zinc-finger enzyme poly(ADP-ribose) polymerase 1 (PARP-1). In the case of TrxR inhibition, their activity depended clearly on the size of the alkyl/aryl residues of phosphorus atoms. Density functional theory (DFT) calculations showed that the Au–P bond of the triphenylphosphane complex $[Au^{I}(NHC)(PPh_3)]I$ had a lower bond dissociation energy compared to trialkylphosphane complexes $[Au^{I}(NHC)(PR_3)]I$, indicating a higher kinetic reactivity of this particular compound. In fact, $[Au^{I}(NHC)(PPh_3)]I$ triggered an enhanced inhibitory activity against PARP-1.

Introduction

Related to the interesting therapeutic profile of the antiarthritic coordination compound auranofin [(1-thio-β-D-glucopyranose-2,3,4,6-tetraacetato-*S*)(triethylphosphine) gold(I)); Figure 1] and other gold(I) complexes, the study of the medicinal properties of gold compounds experienced a renaissance over the last decades.[1] In fact, auranofin and various other gold phosphane complexes show significant antitumor properties, both in vitro and in vivo.[2] Much effort has been directed towards understanding the mode of action of this class of cytotoxic agents and their preferred protein targets, as it has become increasingly evident that DNA interaction is not the unique mode of action of these metallodrugs.[3]

Nowadays organometallic gold complexes have attracted major attention as potential novel antitumor agents including species with N-heterocyclic carbenes (NHCs)[4] or alkynyls[5] as coordinated ligands.[6] The interest in the medicinal chemistry of gold NHC complexes is due to a number of findings, including the fact that they trigger strong cytotoxic effects, induce apoptosis, and inhibit crucial enzymes for the maintenance of the intracellular redox balance, such as the tumor-relevant disulfide reductase enzyme thioredoxin reductase (TrxR).[7] The inhibition of TrxR by gold(I) compounds (including NHC species) has been suggested to occur via direct binding of gold to the selenocystein residue in the enzyme active site, and it is nowadays considered to play a central role in the overall activity of this class of drug candidates.[4a,8]

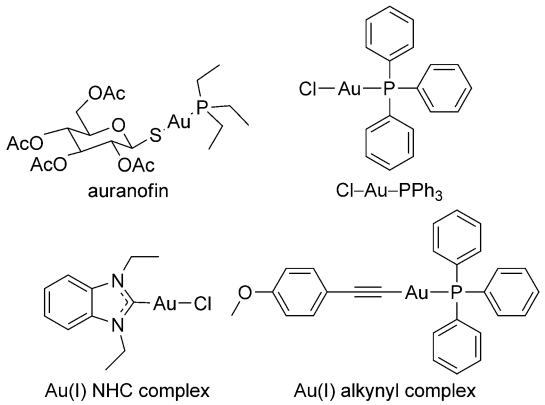

Figure 1. Examples of bioactive gold complexes.

Recently, we have identified NHC complexes of the type $[Au^{I}(NHC)(PR_3)]^{+}$ as a particularly interesting type of gold organometallics that induces cytotoxicity and apoptosis through different pathways.[4c,8c] These compounds were shown to inhibit TrxR, perturb the cellular redox balance and affect the mitochondrial biochemistry. Notably, the phosphane moiety included in the complexes represents one of the most intensively studied ligands of bioactive gold complexes and is also pres-

[a] *Dr. R. Rubbiani, Prof. Dr. I. Ott*
Institute of Medicinal and Pharmaceutical Chemistry
Technische Universität Braunschweig
Beethovenstrasse 55, 38106 Braunschweig (Germany)
E-mail: ingo.ott@tu-bs.de

[b] *Dr. L. Salassa*
CIC biomaGUNE
Paseo Miramón 182, 20009 Donostia, Euskadi (Spain)

[c] *Dr. L. Salassa*
Kimika Fakultatea, Euskal Herriko Unibertsitatea and
Donostia International Physics Center (DIPC)
P.K. 1072, 20080 Donostia, Euskadi (Spain)

[d] *A. de Almeida, Prof. A. Casini*
Department of Pharmacokinetics, Toxicology and Targeting
Research Institute of Pharmacy, Rijksuniversiteit Groningen
Antonius Deusinglaan 1, 9713AV Groningen (The Netherlands)

Supporting information for this article is available on the WWW under http://dx.doi.org/10.1002/cmdc.201400056.

ent in the lead compound auranofin.[9] However, it should be mentioned that a general direct correlation between TrxR inhibition and cytotoxic effects of gold NHC complexes could so far not always be claimed, and this indicates that other mechanisms besides TrxR inhibition might contribute to the overall pharmacological profile.[10]

In this paper we report on the synthesis and characterization of a new series of [Au^{I}(NHC)(PR_3)]I complexes with different alkyl residues at the phosphorus atom. The compounds have been screened for their antiproliferative properties in human cancer cell lines in comparison to a derivative containing the triphenylphosphane moiety, which had been investigated in our previous reports.[4c,8c] This structural modification leads to major changes in the biological activity and cellular bioavailability, as assessed using atomic absorption spectroscopy. In order to gain insight into the possible intracellular targets, the compounds were tested for the inhibition of TrxR and of the enzyme glutathione reductase (GR), a pyridinedisulfide oxidoreductase which maintains glutathione in its reduced state and displays an extended structural similarity with TrxR. Moreover, in this study we report on the possible inhibition by the new compounds of the enzyme poly(ADP-ribose) polymerase I (PARP-1).

PARPs are zinc-finger proteins, and their role in DNA repair by detecting DNA strand breaks and catalyzing poly(ADP-ribosylation) is essential in cancer, particularly in cancer resistance to chemotherapies.[11] It has been shown that gold ions can be incorporated in the zinc-finger domains of transcription factors,[12] and recently, some of us reported on the potent inhibition of PARP-1 by gold(I) phosphane complexes.[13] Additionally, density functional theory (DFT) studies were performed to correlate the biological properties of the new compounds to descriptors obtained by computational chemistry.

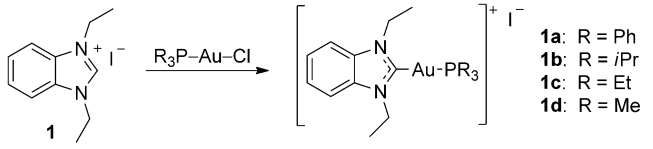

Scheme 1. Synthesis of gold(I) NHC phosphane complexes.

Results

Synthesis and computational chemistry

The synthesis of 1,3-diethylbenzimidazol-2-ylidene gold(I) phosphane complexes was achieved following an established method with opportune modifications (see Scheme 1).[4c] Benzimidazolium iodide was dissolved in dichloromethane in presence of Na_2CO_3. The suspension was heated at 50 °C for 10 min, the respective chlorido gold(I) trialkylphosphane was added, and the mixture was kept at room temperature for 60 h. The target complexes were isolated and purified by filtration, extraction and recrystallization.

Characteristic spectroscopic features that indicate the formation of the complexes included the absence of the C^2 proton signal at $\delta = 8$–10 ppm in the ^{1}H NMR spectra, the shift of the C^2 signal in the ^{13}C NMR spectra from $\delta = 141$ ppm (in the spectrum of benzimidazolium iodide) to $\delta = 192$ ppm (in the spectra of the complexes), the presence of the cationic signal in ESI-MS positive mode, as well as singlet signals in ^{31}P NMR spectra. The high purity of the complexes was confirmed by elemental analysis with deviations from the theoretical values of lower than 0.4%.

Density functional theory (DFT) was employed to identify possible correlations between biological activities and chemical properties of the complexes. Geometry optimization and binding energy (BDE) calculations were performed on **1a–d** using three different functionals (PBE0,[14] CAM-B3LYP[15] and M062X),[16] the SDD effective core potential[17] for Au and the 6-31+G** basis set[18] for the other atoms. Solvent (H_2O) effects were introduced employing the PCM model[19] and BDEs were calculated correcting the basis set superimposition error (BSSE) by the counterpoise method.[20] For the sake of brevity, discussion on BDEs is limited to PBE0, since all functionals provide similar results and PBE0 has the lowest BSSE values (3.9–15.6%). Selected orbitals and electrostatic potential surfaces were also calculated and are reported in Figure 2 and the Supporting Information together with a full account on other computational data.

As shown in Table 1, all four complexes display similar bond lengths and linear coordination geometry. More interestingly, comparison of BDE values highlights that the Au–PR_3 bond stability in **1a** is significantly lower than for the other com-

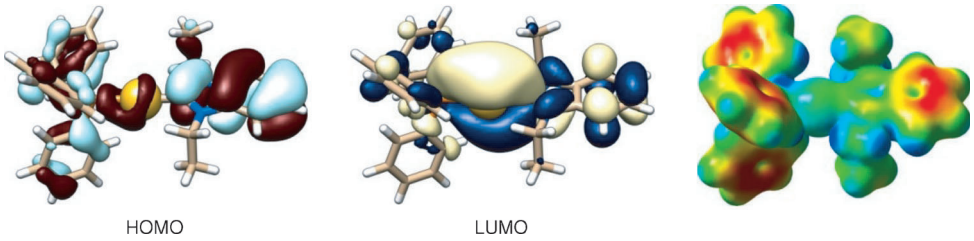

Figure 2. HOMO and LUMO orbitals and electrostatic potential surface (EPS) for complex **1a** calculated with the M062X functional in H_2O (PCM). EPS surfaces are shown in both space and mapped on electron density (isovalue 0.01) of the molecules. The electrostatic potential is represented with a color scale going from red (0.08 a.u.) to blue (0.2 a.u.).

Table 1. Selected bond distances [Å], angles [°] and BDE values [kJ mol^{-1}] for **1a–d** calculated by DFT at the PBE0/SDD/6-31+G** level and using the PCM solvent model (H_2O).

Complex NHC–Au–PR_3	Au–P [Å]	Au–C [Å]	P–Au–C [°]	BDE [kJ mol^{-1}] NHC–Au	Au–PR_3
1a	2.333	2.047	179.2	247.4	137.0
1b	2.341	2.052	178.8	231.3	210.6
1c	2.331	2.052	179.9	233.1	213.7
1d	2.327	2.050	179.8	235.7	214.8

pounds, likely resulting in higher reactivity and different biological activity (see below). Such value is in good agreement with data previously reported and obtained with a different method.[4c] Among complexes **1a–d**, differences in the NHC–Au bond stability are less pronounced. No direct correlation between the Au–P bond strength and the phosphine cone angle is found, having $\theta = 145^\circ$ for PPh_3, $\theta = 162^\circ$ for $P(iPr)_3$, $\theta = 132^\circ$ for PEt_3, and $\theta = 118^\circ$ for PMe_3. The different stability of **1a** must probably be sought in the delicate balance between electron donating and electron accepting properties of the NHC and PR_3 ligands. Compared to other five-membered ring NHC ligands (good σ donors and poor π acceptors), the one used in this work should display better π-accepting properties which match with better σ-donating phosphines such as in **1b–d**, hence explaining the lower stability of the Au–PPh_3 moiety.

All complexes show a flat color distribution in the electrostatic potential surfaces (EPSs), consistent with their relatively nonpolar nature. As shown for **1a** (Figure 2), the HOMO is mainly centered on the phosphane and NHC ligands whereas the LUMO has bonding character over the NHC–Au–PR_3 axis.

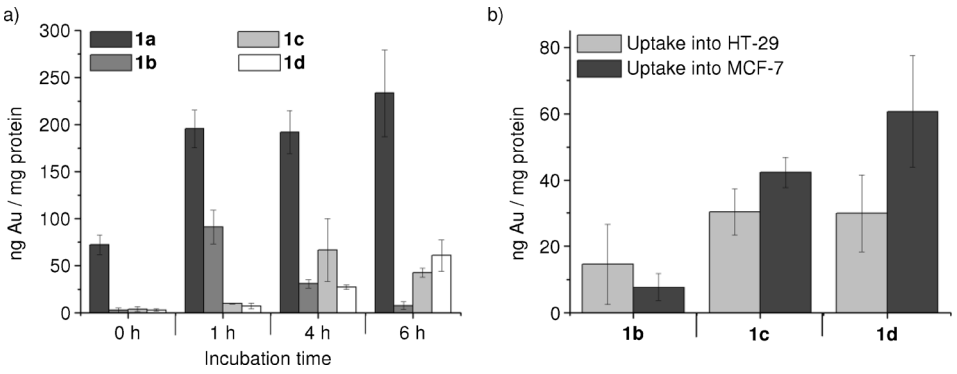

Figure 3. a) Time-dependent cellular gold uptake into MCF-7 cells treated with 3.0 μM of **1a–d**; b) cellular uptake of 3 μM of complexes **1b–d** into MCF-7 and HT-29, after 6 h of incubation.

Antiproliferative effects and cellular uptake

Initially, the gold(I) NHC complexes were tested for their antiproliferative effects in MCF-7 human breast adenocarcinoma and HT-29 human colon adenocarcinoma cells using an established assay.[4c] As expected, low IC_{50} values (all < 10 μM) for cytotoxicity were reached in both cell lines with a clear preference for growth inhibition of MCF-7 cells compared to HT-29 cells. The most active compound of the series is **1a**, bearing the triphenylphosphane moiety, with IC_{50} values in the nanomolar range.

The cellular gold uptake into MCF-7 breast cancer cells exposed to **1a–d** was measured by high-resolution continuum source atomic absorption spectroscopy (HR-CS-AAS) in order to evaluate the influence of the respective phosphane partial structure on the cellular bioavailability.[4c] The obtained results are reported in Figure 3. The highest cellular accumulation was observed with the triphenylphosphane derivative **1a**, whereas the trialkylphosphanes **1b–d** showed significantly lower cellular gold levels. Obviously this effect appears to be related to the high lipophilicity of the triphenylphosphane partial structure of **1a**. Complex **1b** showed highest levels after 1 h, which quickly decreased over time. In contrast, the uptake of **1c** and **1d** was slower and increased over time.

In order to check if the increased cytotoxicity against MCF-7 cells (see above) correlates to a higher accumulation in these cells, comparative experiments using MCF-7 and HT-29 cells were performed with complexes **1b–d**. However, these studies did not provide a clear trend since the values were comparable in both cell lines in the case of **1b** but slightly elevated in MCF-7 cells exposed to **1c** and **1d**.

Enzyme inhibition studies

The inhibition of the activity of the target enzyme TrxR by the gold(I) NHC phosphane complexes **1a–d** was determined using an established assay (see Table 2). Glutathione reductase (GR) was also tested as a closely related (but non-selenocysteine-containing) enzyme to check for TrxR specificity of the enzymatic inhibition. Values for the gold-free benzimidazolium iodide **1** (inactive) and auranofin (high activity) were added to Table 2 as negative and positive references, respectively.[4c]

The $[Au^I(NHC)(PR_3)]I$ complexes **1a–d** efficiently inhibited the target enzyme TrxR with IC_{50} values reaching the nanomolar range. Interestingly, decreasing the size of the residues of the phosphane ligand was accompanied by a significant increase in the efficacy of TrxR inhibition with an overall order of **1a** < **1b** < **1c** ≈ **1d**. In fact, the most potent TrxR inhibitors **1c** and **1d** were of comparable activity with the established lead compound auranofin and also showed an appreciable selectivity over GR inhibition of > 80-fold, which exceeded that of recently studied gold NHC derivatives.[4b,c,10a] Auranofin, however, reaches substantially higher selectivity.[4c,21]

Table 2. IC_{50} values [μM] for inhibition of TrxR, GR, PARP-1 and cell proliferation of HT-29 and MCF-7 cells by **1**, **1a–d** and auranofin.

	IC_{50} [μM][a]				
Compd	HT-29	MCF-7	TrxR	GR	PARP-1
1	> 100	> 100	> 50	> 50	n.d.
1a[4c]	0.89 ± 0.40	0.41 ± 0.18	0.66 ± 0.02	2.60 ± 0.55	0.04 ± 0.01
1b	5.98 ± 1.78	0.59 ± 0.23	0.11 ± 0.06	4.72 ± 0.53	0.45 ± 0.03
1c	8.85 ± 2.1	0.81 ± 0.07	0.03 ± 0.00	2.55 ± 0.12	0.40 ± 0.05
1d	1.46 ± 0.19	0.74 ± 0.49	0.03 ± 0.01	3.42 ± 1.62	0.40 ± 0.10
auranofin	2.60 ± 0.40	1.10 ± 0.33	0.01 ± 0.00	15.00 ± 0.10	0.08 ± 0.01

[a] Data are the mean ± SEM of two to three independent experiments each performed with $n = 6$ for cytotoxicity and $n = 3$ for enzyme inhibition measurements.

Afterwards, the ability of the new compounds to inhibit the zinc-finger enzyme PARP-1 was determined on the purified human enzyme according to established procedures (see Experimental Section for details). For this purpose, the enzyme was incubated with each compound at various concentrations for 1 h before assessing its activity spectrophotometrically by measuring the incorporation of biotinylated poly(ADP-ribose) into histone proteins. The resulting IC_{50} values for PARP-1 inhibition are reported in Table 2. All complexes displayed inhibitory activity towards PARP-1 with IC_{50} values in the sub-micromolar range. Notably, **1a**–**d** are superior (around 100-fold) PARP-1 inhibitors compared to 3-aminobenzamide (3-AB, benchmark PARP-1 inhibitor, $IC_{50} = 33\ \mu M$[13a]). The most active complexes were **1a** and auranofin, which were approximately 5–10-fold more active than **1b**–**d**. The higher reactivity of **1a** compared to the other complexes is consistent with its lowest BDE value for the Au–PR_3 bond.

Conclusions

A series of gold(I) N-heterocyclic carbene phosphane complexes has been synthesized and structurally characterized. All the complexes induced antiproliferative effects towards two cancer cell lines (HT-29 and MCF-7) with low IC_{50} values in the micromolar and sub-micromolar range. To some extent, the bioactivities were correlated to the extent of cellular accumulation. Complex **1a** with the triphenylphosphane partial structure had the most efficient uptake. Of note, the cellular uptake enhancing effect of the triphenylphosphane moiety in comparison with trialkylphosphanes had already been observed for gold(I) complexes of the type $Au^{I}Cl(PR_3)$.[9d] In a previous report it was shown that the high cellular uptake of **1a** was also accompanied by an elevated transport into mitochondria and a triggering of strong antimitochondrial effects.[4c] This could also be of relevance for **1b**–**d** and might at least in part be related to the cationic nature of the complexes, since antimitochondrial effects of cationic gold NHC complexes are well established.[4c, 22]

As expected, all complexes displayed low IC_{50} values concerning inhibition of TrxR, which can be considered to be one of the main cellular targets for **1a**–**d**. Decreasing the size of the residues at the phosphorus atom led to stronger inhibition of TrxR. In particular, complexes **1c** and **1d** represent highly active and very selective TrxR inhibitors. PARP-1 was identified as an additional important target of the bioactivity of $[Au^{I}(NHC)(PR_3)]$ complexes. The triphenylphosphane complex **1a** afforded the highest activity, and it can be concluded that for this particular compound the interaction with PARP-1 may also be of relevance, although further studies assessing enzyme inhibition directly on cell extracts should be performed to validate this hypothesis. Moreover, DFT calculations indicated that this enhanced activity could be the consequence of higher reactivity with respect to ligand exchange reactions of **1a** (lower BDE).

In summary, $[Au^{I}(NHC)(PR_3)]$ complexes represent an interesting class of bioorganometallics and exhibit relevant key features for the design of active metal-based anticancer agents. Further investigations on the biological and medicinal chemistry as well as on their kinetic properties are ongoing.

Experimental Section

General

All reagents and the solvents were used as received from Sigma–Aldrich, Acros Organics, Invitrogen or other commercial suppliers. ^1H NMR, ^{13}C NMR and ^{31}P NMR were recorded on a Bruker DRX-400 AS, mass spectra were recorded on a Finnigan MAT 4515 and an LTQ XL instrument (Thermo Electron Corp.). The syntheses of 1,3-diethylbenzimidazolium iodide (**1**) and (1,3-diethylbenzylimidazol-2-ylidene)gold(I)triphenylphosphane iodide (**1a**) have been previously reported.[4b,c] MCF-7 breast adenocarcinoma and HT-29 colon adenocarcinoma cells were maintained in Dulbecco's modified Eagle's medium high glucose (DMEM; PAA Laboratories GmbH), supplemented with 50 mg L^{-1} gentamycin (USBiological) and 10% (*v*/*v*) fetal calf serum (FCS, Biochrom AG) prior to use.

Synthesis

Gold(I) NHC phosphane complexes: 1,3-Diethylbenzimidazolium iodide (0.060 g, 0.2 mmol) was dissolved in CH_2Cl_2 in presence of Na_2CO_3 (0.021 g, 0.2 mmol), heated 10 min at 50 °C and reacted with the respective chlorido(trialkylphosphane) gold(I) (0.2 mmol) under vigorous stirring for 60 h at RT. Na_2CO_3 was removed by filtration, and the respective target complex was purified by liquid/liquid extraction with CH_2Cl_2/H_2O. The organic solvent was evaporated, and the residue was recrystallized in CH_2Cl_2/hexane to give the pure product.

(1,3-Diethylbenzylimidazol-2-ylidene)gold(I)(tri-isopropylphosphane) iodide (1b): White powder (0.071 g, 0.11 mmol, 54%): mp: 174 °C; ^1H NMR ($CDCl_3$): $\delta = 1.34$–1.45 (m, 18H, $PCH(\underline{CH_3}_2)$), 1.67 (t, 6H, $^3J = 7.4$ Hz, CH_3), 2.60–2.64 (m, 3H, $P\underline{CH}(CH_3)_2$), 4.71 (q, 4H, $^3J = 7.4$ Hz, CH_2), 7.49 (dd, 2H, $^4J = 3.1$ Hz, $^3J = 6.2$ Hz, $ArH_{4/7}$), 7.59 ppm (dd, 2H, $^4J = 3.1$ Hz, $^3J = 6.2$ Hz, $ArH_{5/6}$); ^{13}C NMR ($CDCl_3$): $\delta = 16.0$ (CH_3), 20.3 ($PCH(\underline{CH_3}_2)$), 20.6 ($P\underline{CH}(CH_3)_2$), 44.2 (CH_2), 111.6 ($ArC^{3a/7a}$), 124.7 (ArC^4), 133.0 (ArC^5), 192.6 ppm (ArC^2); ^{31}P NMR ($CDCl_3$): $\delta =$ 66.0 ppm; MS (ESI): *m*/*z*: 531 $[M-I]^+$; Anal. calcd for $C_{20}H_{35}AuN_2P{\cdot}I$: C 36.49, H 5.36, N 4.26, found: C 36.66 H 5.42 N 4.48.

(1,3-Diethylbenzylimidazol-2-ylidene)gold(I) triethylphosphane iodide (1c): White powder (0.073 g, 0.12 mmol, 59%): mp: 215 °C; ^1H NMR ($CDCl_3$): $\delta = 1.15$–1.25 (m, 9H, $PCH_2\underline{CH_3}$), 1.65 (t, 6H, $J = 7.4$ Hz, CH_3), 1.87–1.98 (m, 6H, $P\underline{CH_2}CH_3$), 4.72 (q, 4H, $^3J = 7.3$ Hz, CH_2), 7.48 (dd, 2H, $^4J = 3.1$ Hz, $^3J = 6.2$ Hz, $ArH_{4/7}$), 7.57 ppm (dd, 2H, $^4J = 3.1$ Hz, $^3J = 6.2$ Hz, $ArH_{5/6}$); ^{13}C NMR ($CDCl_3$): $\delta = 8.9$ ($PCH_2\underline{CH_3}$), 15.6 (CH_3), 17.8 ($P\underline{CH_2}CH_3$), 44.2 (CH_2), 111.6 ($ArC^{3a/7a}$), 124.7 (ArC^4), 133.1 (ArC^5), 190.3 ppm (ArC^2); ^{31}P NMR ($CDCl_3$): $\delta = 39.4$ ppm; MS (EI): *m*/*z*: 489 $[M-I]^+$; Anal. calcd for $C_{17}H_{29}AuN_2P{\cdot}I$: C 33.13, H 4.74, N 4.55, found: C 33.44, H 4.61, N 4.29.

(1,3-Diethylbenzylimidazol-2-ylidene)gold(I) trimethylphosphane iodide (1d): White powder (0.057 g, 0.08 mmol, 49%): mp: 196 °C; ^1H NMR ($CDCl_3$): $\delta = 1.65$–1.75 (m, 15H, PCH_3/CH_3), 4.71 (q, 4H, $J = 7.3$ Hz, CH_2), 7.48 (dd, 2H, $^4J = 3.1$ Hz, $^3J = 6.2$ Hz, $ArH_{4/7}$), 7.60 ppm (dd, 2H, $^4J = 3.1$ Hz, $^3J = 6.2$ Hz, $ArH_{5/6}$); ^{13}C NMR ($CDCl_3$): $\delta = 14.9$ (PCH_3), 16.0 (CH_3), 44.2 (CH_2), 111.6 ($ArC_{3a/7a}$), 124.8 ($ArC_{5/6}$), 133.0 ($ArC_{4/7}$), 189.9 ppm (NHC); ^{31}P NMR ($CDCl_3$): $\delta = 39.3$ ppm; MS (ESI) : *m*/*z*: 447 $[M-I]^+$; Anal. calcd for $C_{14}H_{23}AuN_2P{\cdot}I$: C 29.28, H 4.04, N 4.88, found: C 29.66, H 4.06, N 5.00.

Computational chemistry

All density functional theory (DFT) calculations were performed employing the Gaussian 09 (G09) program.[23] Geometry optimization calculations were performed on complexes **1a–d** using the PBE0, CAM-B3LYP[14,15] and M062X[16] functionals together with the SDD effective core potential[17] (Au) and the 6-31+G** (P, O, N, C, H) basis set.[17] In all cases the structures were calculated including solvent effects (H_2O) by means of the PCM model.[17] In the case of the PBE0 functional calculation in the gas phase were also performed. The nature of all stationary points was confirmed by normal mode analysis.

The binding energy (BDE) for the phosphine ligands was calculated as $BDE = E_{(NHC\text{-}Au\text{-}P)} - E_{(NHC\text{-}Au)} - E_{(P)}$, where $E_{(NHC\text{-}Au\text{-}P)}$, $E_{(NCH\text{-}Au)}$, and $E_{(P)}$ represent the total energy of complexes **1a–d**, of the NCH–Au and phosphine ligand fragments, respectively. The same approach was adopted to calculate the BDE for the two NHC ligands. Basis set superposition error (BSSE)[20a,b] was corrected by the counterpoise method of Boys and Bernardi.[20c]

Biology

Antiproliferative effects in MCF-7 and HT-29 cells: The antiproliferative effects in MCF-7 and HT-29 cells after 72 h (HT-29) or 96 h (MCF-7) exposure to the gold complexes were evaluated according to a procedure already described in [4b]. For the experiments, the compounds were prepared freshly as stock solutions in *N*,*N*-dimethylformamide (DMF) and diluted with the cell culture medium to the final assay concentrations (0.1% *v/v* DMF). The cells were routinely cultured in a 75 cm^2 flask with 10 mL of cell culture medium. For the assay, the cells were seeded (10000 cells mL^{-1} for MCF-7 and 5000 cells mL^{-1} for HT-29) into 96-well plates and incubated at 37 °C with 5% CO_2. After exposure to the complexes for 72 h (HT-29) or 96 h (MCF-7), cells were stained with crystal violet, and the absorbance was measured at 595 nm in a microplate reader (VictorX4, PerkinElmer). The IC_{50} values were calculated as the concentrations reducing proliferation of untreated control cells by 50% and are given as the means ± standard error of the mean of at least two independent experiments (each performed with $n=6$).

Cellular uptake: MCF-7 breast cancer cells were grown until at least 80% confluence in 75 cm^2 uptake cell culture flasks. Stock solutions of 3.0 mM of the gold complexes in DMF were freshly prepared and diluted (1:1000) with culture medium supplemented with 10% (*v/v*) FCS. The cell culture medium of the flasks was replaced with medium containing the substances and incubated for 0, 1, 4 and 6 h at 37 °C/5% CO_2. The intact cell pellets were collected after trypsinisation (0.05% trypsin) and centrifugation (3000 g, 5 min.). Cell pellets were treated with 1000 μL lysis buffer (Tris-HCl 10 mM, NaCl 10 mM, $MgCl_2$ 10 mM, pH 7.4) for 20 min on ice and lysed in a pre-chilled dounce homogenisator. A 20 μL aliquot of the lysate was removed for protein quantification by the Bradford method, and another 100 μL aliquote was diluted to 200 μL supplemented with 20 μL of Triton X 100 (1%) and investigated by AAS (see below). Results were expressed as ng gold per mg protein as mean ± standard error of the mean of two independent experiments.

Atomic absorption spectroscopy: Gold contents were measured with a graphite furnace high-resolution atomic absorption spectrometer (contraAA700, Analytik Jena AG, Jena, Germany) at 242.7950 nm according to a recently described method.[4c,24] Matrix-matched calibration with gold standard solutions (Fluka) was used as calibration mode. Probes were injected at a volume of 20 μL into graphite wall tubes. The mean of absorbance of duplicate injections was used throughout the study.

TrxR/GR inhibition assay: To determine the inhibition of TrxR and GR, an established microplate-reader-based assay was performed with minor modifications.[4b] For this purpose commercially available rat liver TrxR and baker yeast GR (both from Sigma–Aldrich) were used and diluted with distilled H_2O to achieve a concentration of 2.0 U mL^{-1}. The compounds were freshly dissolved as stock solutions in DMF. To each 25 μL aliquot of the enzyme solution 25 μL of potassium phosphate buffer pH 7.0 containing the compounds in graded concentrations or vehicle (DMF) without compounds (control probe) was added, and the resulting solutions (final concentration of DMF: max. 0.5% *v/v*) were incubated with moderate shaking for 75 min at 37 °C in a 96-well plate. To each well 225 μL of reaction mixture were added (1000 μL reaction mixture consisted of 500 μL potassium phosphate buffer pH 7.0, 80 μL 100 mM EDTA solution pH 7.5, 20 μL BSA solution 0.05%, 100 μL 20 mM NADPH solution and 300 μL distilled H_2O). The reaction was started by addition of 25 μL of a 20 mM ethanolic 5,5′-dithiobis(2-nitrobenzoic acid) (DTNB) solution. After proper mixing, the formation of 5-thio-2-nitrobenzoic acid (5-TNB) was monitored with a microplate reader (VictortmX4, PerkinElmer) at 405 nm in 10 s intervals for 6 min. The increase in 5-TNB concentration over time followed a linear trend ($r^2 \geq 0.99$), and the enzymatic activities were calculated as the slopes (increase in absorbance per second) thereof. For each tested compound, non-interference with the assay components was confirmed by a negative control experiment using an enzyme-free solution. The IC_{50} values were calculated as the concentration of compound decreasing the enzymatic activity of the untreated control by 50% and are given as the means ± standard error of the mean of three to six independent experiments.

PARP-1 activity determinations: Purified PARP-1 was incubated with various concentrations of compounds for 1 h at RT prior to the assay. PARP-1 activity was then determined using the Trevigen HT Universal Colorimetric PARP Assay (Gaithersburg, MD, USA). This assay measures the incorporation of biotinylated poly(ADP-ribose) onto histone proteins in a 96-microtiter-strip well format. Either recombinant human PARP-1 (high specific activity, purified from *E. coli* containing recombinant plasmid harbouring the human PARP gene, supplied with the assay kit) or an aliquot of protein cell extracts (50 μg) was used as the enzyme source. 3-Aminobenzamide (3-AB), provided in the kit, was used as control inhibitor. Two controls were always performed in parallel: a positive activity control for PARP-1 without inhibitors that provided the 100% activity reference point, and a negative control, without PARP-1, to determine background absorbance. The final reaction mixture (50 μL) was treated with TACS-Sapphire, a horseradish peroxidase colorimetric substrate, and incubated in the dark for 30 min. Absorbance was measured at 630 nm after 30 min.

Acknowledgements

Financial support by Fonds der Chemischen Industrie (FCI), COST action CM1105 and DAAD/Erasmus Teaching Assignment program is gratefully acknowledged. A.C. thanks the University of Groningen (Rosalind Franklin Fellowship) for funding. L.S. was financed by the MICINN of Spain (Ramón y Cajal Fellowship RYC-2011-07787). The SGI/IZO-SGIker UPV/EHU is gratefully acknowledged for generous allocation of computational resources. L.S. is

also grateful to Prof. J. M. Ugalde, Drs. T. Mercero and E. Ogando for their kind support.

Keywords: anticancer compounds · bioorganometallics · gold complexes · N-heterocyclic carbene complexes · poly(ADP-ribose) polymerase 1 · thioredoxin reductase

[1] a) C. F. Shaw, *Chem. Rev.* **1999**, *99*, 2589 – 2600; b) I. Ott, *Coord. Chem. Rev.* **2009**, *253*, 1670 – 1681; c) S. Nobili, E. Mini, I. Landini, C. Gabbiani, A. Casini, L. Messori, *Med. Res. Rev.* **2010**, *30*, 550 – 580; d) S. J. Berners-Price, A. Filipovska, *Metallomics* **2011**, *3*, 863 – 873.

[2] a) E. R. T. Tiekink, *Crit. Rev. Oncol. Hematol.* **2002**, *42*, 225 – 248; b) E. Vergara, A. Casini, F. Sorrentino, O. Zava, E. Cerrada, M. P. Rigobello, A. Bindoli, M. Laguna, P. J. Dyson, *ChemMedChem* **2010**, *5*, 96 – 102; c) E. Vergara, E. Cerrada, C. Clavel, A. Casini, M. Laguna, *Dalton Trans.* **2011**, *40*, 10927 – 10935.

[3] a) A. Casini, L. Messori, *Curr. Top. Med. Chem.* **2011**, *11*, 2647 – 2660; b) C. Gabbiani, L. Messori, *Anti-Cancer Agents Med. Chem.* **2011**, *11*, 929 – 939.

[4] a) J. L. Hickey, R. A. Ruhayel, P. J. Barnard, M. V. Baker, S. J. Berners-Price, A. Filipovska, *J. Am. Chem. Soc.* **2008**, *130*, 12570 – 12571; b) R. Rubbiani, I. Kitanovic, H. Alborzinia, S. Can, A. Kitanovic, L. A. Onambele, M. Stefanopoulou, Y. Geldmacher, W. S. Sheldrick, G. Wolber, A. Prokop, S. Wölfl, I. Ott, *J. Med. Chem.* **2010**, *53*, 8608 – 8618; c) R. Rubbiani, S. Can, I. Kitanovic, H. Alborzinia, M. Stefanopoulou, M. Kokoschka, S. Mönchgesang, W. S. Sheldrick, S. Wölfl, I. Ott, *J. Med. Chem.* **2011**, *54*, 8646 – 8657; d) E. Schuh, C. Pflüger, A. Citta, A. Folda, M. P. Rigobello, A. Bindoli, A. Casini, F. Mohr, *J. Med. Chem.* **2012**, *55*, 5518 – 5528; e) L. Kaps, B. Biersack, H. Muller-Bunz, K. Mahal, J. Munzner, M. Tacke, T. Mueller, R. Schobert, *J. Inorg. Biochem.* **2012**, *106*, 52 – 58; f) T. Zou, C. T. Lum, S. S.-Y. Chui, C.-M. Che, *Angew. Chem.* **2013**, *125*, 3002 – 3005; *Angew. Chem. Int. Ed.* **2013**, *52*, 2930 – 2933; g) F. Hackenberg, H. Müller-Bunz, R. Smith, W. Streciwilk, X. Zhu, M. Tacke, *Organometallics* **2013**, *32*, 5551 – 5560; h) H. Sivaram, J. Tan, H. V. Huynh, *Dalton Trans.* **2013**, *42*, 12421 – 12428.

[5] a) A. Meyer, C. P. Bagowski, M. Kokoschka, M. Stefanopoulou, H. Alborzinia, S. Can, D. H. Vlecken, W. S. Sheldrick, S. Wölfl, I. Ott, *Angew. Chem.* **2012**, *124*, 9025 – 9030; *Angew. Chem. Int. Ed.* **2012**, *51*, 8895 – 8899; b) A. Meyer, A. Gutiérrez, I. Ott, L. Rodríguez, *Inorg. Chim. Acta* **2013**, *398*, 72 – 76; c) E. Schuh, S. M. Valiahdi, M. A. Jakupec, B. K. Keppler, P. Chiba, F. Mohr, *Dalton Trans.* **2009**, 10841 – 10845; d) C.-H. Chui, R. S.-M. Wong, R. Gambari, G. Y.-M. Cheng, M. C.-W. Yuen, K.-W. Chan, S.-W. Tong, F.-Y. Lau, P. B.-S. Lai, K.-H. Lam, C.-L. Ho, C.-W. Kan, K. S.-Y. Leung, W.-Y. Wong, *Bioorg. Med. Chem.* **2009**, *17*, 7872 – 7877.

[6] B. Bertrand, A. Casini, *Dalton Trans.* **2013**, *43*, 4209 – 4219.

[7] a) L. Oehninger, R. Rubbiani, I. Ott, *Dalton Trans.* **2013**, *42*, 3269 – 3284; b) W. Liu, R. Gust, *Chem. Soc. Rev.* **2013**, *42*, 755 – 773; c) F. Cisnetti, A. Gautier, *Angew. Chem.* **2013**, *125*, 12194 – 12196; *Angew. Chem. Int. Ed.* **2013**, *52*, 11976 – 11978.

[8] a) A. Bindoli, M. P. Rigobello, G. Scutari, C. Gabbiani, A. Casini, L. Messori, *Coord. Chem. Rev.* **2009**, *253*, 1692 – 1707; b) S. Urig, K. Fritz-Wolf, R. Reau, C. Herold-Mende, K. Toth, E. Davioud-Charvet, K. Becker, *Angew. Chem.* **2006**, *118*, 1915 – 1920; *Angew. Chem. Int. Ed.* **2006**, *45*, 1881 – 1886; c) A. Pratesi, C. Gabbiani, E. Michelucci, M. Ginanneschi, A. M. Papini, R. Rubbiani, I. Ott, L. Messori, *J. Inorg. Biochem.* **2014**, in press; http://dx.doi.org/10.1016/j.jinorgbio.2014.01.009.

[9] a) M. J. McKeage, L. Maharaj, S. J. Berners-Price, *Coord. Chem. Rev.* **2002**, *232*, 127 – 135; b) O. Rackham, S. J. Nichols, P. J. Leedman, S. J. Berners-Price, A. Filipovska, *Biochem. Pharmacol.* **2007**, *74*, 992 – 1002; c) G. F. Rush, P. F. Smith, G. D. Hoke, D. W. Alberts, R. M. Snyder, C. K. Mirabelli, *Toxicol. Appl. Pharmacol.* **1987**, *90*, 391 – 400; d) H. Scheffler, Y. You, I. Ott, *Polyhedron* **2010**, *29*, 66 – 69.

[10] a) R. Rubbiani, E. Schuh, A. Meyer, J. Lemke, J. Wimberg, N. Metzler-Nolte, F. Meyer, F. Mohr, I. Ott, *MedChemComm* **2013**, *4*, 942 – 948; b) A. Citta, E. Schuh, F. Mohr, A. Folda, M. L. Massimino, A. Bindoli, A. Casini, M. P. Rigobello, *Metallomics* **2013**, *5*, 1006 – 1015.

[11] V. Schreiber, F. Dantzer, J. C. Ame, G. de Murcia, *Nat. Rev. Mol. Cell Biol.* **2006**, *7*, 517 – 528.

[12] a) M. A. Franzman, A. M. Barrios, *Inorg. Chem.* **2008**, *47*, 3928 – 3930; b) M. L. Handel, A. deFazio, C. K. Watts, R. O. Day, R. L. Sutherland, *Mol. Pharmacol.* **1991**, *40*, 613 – 618.

[13] a) F. Mendes, M. Groessl, A. A. Nazarov, Y. O. Tsybin, G. Sava, I. Santos, P. J. Dyson, A. Casini, *J. Med. Chem.* **2011**, *54*, 2196 – 2206; b) M. Serratrice, M. A. Cinellu, L. Maiore, M. Pilo, A. Zucca, C. Gabbiani, A. Guerri, I. Landini, S. Nobili, E. Mini, L. Messori, *Inorg. Chem.* **2012**, *51*, 3161 – 3171.

[14] J. P. Perdew, K. Burke, M. Ernzerhof, *Phys. Rev. Lett.* **1996**, *77*, 3865 – 3868.

[15] T. Yanai, D. Tew, N. Handy, *Chem. Phys. Lett.* **2004**, *393*, 51 – 57.

[16] Y. Zhao, D. G. Truhlar, *Theor. Chem. Acc.* **2008**, *120*, 215 – 241.

[17] P. Fuentealba, H. Preuss, H. Stoll, L. v. Szentpaly, *Chem. Phys. Lett.* **1982**, *89*, 418 – 422.

[18] R. Ditchfield, W. J. Hehre, J. A. Pople, *J. Chem. Phys.* **1971**, *54*, 724.

[19] D. M. York, M. Karplus, *J. Phys. Chem. A* **1999**, *103*, 11060 – 11079.

[20] a) N. R. Kestner, *J. Chem. Phys.* **1968**, *48*, 252; b) P. Salvador, S. Simon, M. Duran, J. J. Dannenberg, *J. Chem. Phys.* **2000**, *113*, 5666; c) S. F. Boys, F. Bernardi, *Mol. Phys.* **1970**, 553.

[21] S. Gromer, L. D. Arscott, C. H. Williams, R. H. Schirmer, K. Becker, *J. Biol. Chem.* **1998**, *273*, 20096 – 20101.

[22] a) M. Baker, P. J. Barnard, S. J. Berners-Price, S. K. Brayshaw, J. L. Hickey, B. W. Skelton, A. H. White, *Dalton Trans.* **2006**, 3708 – 3715; b) P. J. Barnard, M. V. Baker, S. J. Berners-Price, D. A. Day, *J. Inorg. Biochem.* **2004**, *98*, 1642 – 1647.

[23] Gaussian 09 (Revision B.01, 2009), M. J. Frisch, G. W. Trucks, H. B. Schlegel, G. E. Scuseria, M. A. Robb, J. R. Cheeseman, G. Scalmani, V. Barone, B. Mennucci, G. A. Petersson, H. Nakatsuji, M. Caricato, X. Li, H. P. Hratchian, A. F. Izmaylov, J. Bloino, G. Zheng, J. L. Sonnenberg, M. Hada, M. Ehara, K. Toyota, R. Fukuda, J. Hasegawa, M. Ishida, T. Nakajima, Y. Honda, O. Kitao, H. Nakai, T. Vreven, J. J. A. Montgomery, J. E. Peralta, F. Ogliaro, M. Bearpark, E. B. J. J. Heyd, K. N. Kudin, V. N. Staroverov, R. Kobayashi, J. Normand, K. Raghavachari, A. Rendell, J. C. Burant, S. S. Iyengar, J. Tomasi, M. Cossi, N. Rega, J. M. Millam, M. Klene, J. E. Knox, J. B. Cross, V. Bakken, C. Adamo, J. Jaramillo, R. Gomperts, R. E. Stratmann, O. Yazyev, A. J. Austin, R. Cammi, C. Pomelli, J. W. Ochterski, R. L. Martin, K. Morokuma, V. G. Zakrzewski, G. A. Voth, P. Salvador, J. J. Dannenberg, S. Dapprich, A. D. Daniels, Ö. Farkas, J. B. Foresman, J. V. Ortiz, J. Cioslowski, D. J. Fox, Gaussian, Inc., Wallingford CT, **2009**.

[24] I. Ott, H. Scheffler, R. Gust, *ChemMedChem* **2007**, *2*, 702 – 707.

Received: January 24, 2014
Published online on March 26, 2014